Cell Death and Differentiation (2010) 17, 408–420

www.nature.com/cdd

Involvement of cytochrome *c* oxidase subunits Va and Vb in the regulation of cancer cell metabolism by Bcl-2

ZX Chen[1,2] and S Pervaiz*[,1,2,3,4]

Bcl-2 has been shown to promote survival of cancer cells by maintaining a slight pro-oxidant state through elevated mitochondrial respiration during basal conditions. On oxidative stress, Bcl-2 moderates mitochondrial respiration through cytochrome *c* oxidase (COX) activity to prevent an excessive buildup of reactive oxygen species (ROS) by-production from electron transport activities. However, the underlying molecular mechanism(s) of Bcl-2-mediated ROS regulation and its impact on carcinogenesis remain unclear. In this study, we show that Bcl-2 expression positively influences the targeting of nuclear-encoded COX Va and Vb to the mitochondria of cancer cells. In addition, evidence is presented in support of a protein–protein interaction between COX Va and Bcl-2, involving the BH2 domain of Bcl-2. Interestingly, episodes of serum withdrawal, glucose deprivation or hypoxia aimed at inducing early oxidative stress triggered Bcl-2-overexpressing cells to preserve mitochondrial levels of COX Va while depressing COX Vb, whereas the reverse was observed in mock-transfected cells. The unique manner in which Bcl-2 adjusted COX subunits during these physiological stress triggers had a profound impact on the resultant decrease in COX activity and maintenance of mitochondrial ROS levels, thus delineating a novel mechanism for the homeostatic role of Bcl-2 in the redox biology and metabolism of cancer cells.
Cell Death and Differentiation (2010) **17,** 408–420; doi:10.1038/cdd.2009.132; published online 16 October 2009

Introduction

The onset and maintenance of the cancer phenotype is orchestrated by a combination of dysregulated cellular pathways that contribute to a resistant environment favorable for cancer cells to thrive in. Recent literature has expounded on the intricate controls behind cancer metabolism, ranging from the emerging nontranscriptional role of p53 to the expanding reach of HIF-1 involvement in the field.[1,2] Despite their multiple roles, the stark similarity lies in their connection to cytochrome *c* oxidase (COX) and its regulation, signaling the dawn of the Warburg effect-revisited era.

Cytochrome *c* oxidase is the terminal complex of the electron transport chain and is located in the inner mitochondrial membrane. COX exists as a dimer, consisting of 13-subunit monomers. The core subunits of COX (subunits I, II and III) are encoded by the mitochondrial genome. The remaining 10 subunits are encoded by the nuclear genome. The nuclear-encoded subunits that surround the catalytic core of COX were shown to be involved in the assembly, stability and dimerization of the enzyme.[3,4] In yeast, the expression of COX IV and VI was shown to be aerobically regulated, whereby the amount of fully assembled COX decreases with decreasing oxygen concentration.[5–8] In the mammalian system, these COX subunits are designated as COX Vb and Va, respectively. During the assembly of COX in mammalian cells, COX Va is incorporated, followed by COX Vb, suggesting that COX Va may determine the integration of COX Vb and that the subsequent addition of COX Vb may have a vital role in COX enzymatic activity.[9,10]

Interestingly, recent studies have demonstrated an upregulation and an increased involvement of COX Va and Vb in a variety of cancers, such as colorectal cancer, squamous cell cancer of the larynx, intraductal carcinoma of the breast and prostate cancer.[11–16] In addition, upregulation of COX Vb has been observed in energy-demanding cell types and healthy tissues; is shown to inhibit apoptosis in intestinal epithelial cells; and is associated with an increase in COX activity in cervical (HeLa) and lung carcinoma cells (A549).[12,17,18] Although the precise regulatory mechanisms and functional roles of these COX subunits in oncogenesis have yet to be elucidated, extensive studies from their yeast homologs, as well as their physiological roles in normal mammalian cells, may suggest similar functions in the mitochondria of cancer cells by enhancing the availability and stability of the final enzyme, thus exerting profound effects on the resultant activity. COX activity influences the overall rates of mitochondrial respiration and electron transport, processes that are not completely efficient, resulting in the generation of superoxide (O_2^-) as a by-product and creating a pro-oxidant milieu to

[1]Department of Physiology, Yong Loo Lin School of Medicine, National University of Singapore, Singapore; [2]NUS Graduate School for Integrative Sciences and Engineering, National University of Singapore, Singapore; [3]Duke-NUS Graduate Medical School, Singapore and [4]Singapore-MIT Alliance, Singapore
*Corresponding author: S Pervaiz, Department of Physiology, MD9 01-05, Yong Loo Lin School of Medicine, National University of Singapore, Singapore 117597, Singapore. Tel: +65 65166602 or +65 96614732; Fax: +65 67788161; E-mail: phssp@nus.edu.sg
Keywords: Bcl-2; superoxide; COX; ROS; cancer
Abbreviations: ATP, adenosine triphosphate; Bak, Bcl-2 antagonist/killer-1; Bax, Bcl-2 associated X protein; Bcl-2, B-cell lymphoma/leukemia-2; BN-PAGE, blue native polyacrylamide gel electrophoresis; COX, cytochrome c oxidase; CuZn SOD, copper/zinc superoxide dismutase; HIF-1, hypoxia-inducible factor 1; O2-, superoxide; RLU, relative light unit; ROS, reactive oxygen species; Tom20, translocase of outer membrane 20
Received 04.3.09; revised 14.7.09; accepted 27.7.09; Edited by L Scorrano; published online 16.10.09

facilitate an extensive array of downstream reactive oxygen species (ROS)-mediated signaling pathways.[19–21]

Bcl-2 is an anti-apoptotic protein, first discovered as a reciprocal gene translocation in chromosome 14 and 18 of follicular lymphomas. Its main site of action and localization lies on the outer mitochondrial membrane and its protective mechanisms center on preserving mitochondrial membrane integrity, preventing cytochrome *c* release and sequestrating pro-apoptotic proteins such as Bax and Bak.[22,23] We previously reported that overexpression of Bcl-2 was associated with a slight increase in intracellular O_2^- production, and reduction of O_2^- sensitized Bcl-2-overexpressing cells to apoptotic stimuli.[20] More recently, we reported a novel, noncanonical role of Bcl-2 in amplifying mitochondrial respiration and COX activity in tumor cells, which is linked to the slight pro-oxidant activity of Bcl-2.[19,20,24,25] Intriguingly, Bcl-2 has also been shown to maintain the slight pro-oxidant state during periods of stress through metabolic adaptations by regulating COX activity and mitochondrial respiration, suggesting a novel anti-apoptotic role of Bcl-2 in conferring resistance to cancer cells.[25] In this study, we tested the hypothesis that Bcl-2 regulation of COX activity was mediated by COX Va and Vb. Indeed, we report an increase in COX Va and Vb localization in the mitochondria of Bcl-2-overexpressing CEM cells during normal conditions and alterations in the composition of these subunits within the mitochondria during bouts of oxidative stress.

Results

Bcl-2 increases O_2^- production through increased mitochondrial respiration in cancer cells. Similar to our earlier reports, we detected consistently higher levels of intracellular O_2^- in Bcl-2-overexpressing CEM cells (1.27 ± 0.08-fold) compared with CEM/Neo cells (Figure 1a). Similarly, using a fluorescent probe for mitochondrial O_2^- (MitoSOX), higher levels of O_2^- were detected in the mitochondria of CEM/Bcl-2 cells compared with CEM/Neo cells, which was corroborated by the lucigenin-based assay performed on isolated mitochondria from both cell lines (Bcl-2 $>$ Neo by 1.71 ± 0.01-fold) (Figure 1b, c). In agreement with our recent findings, CEM/Bcl-2 cells showed a higher COX activity than did CEM/Neo cells by 2.49 ± 1.04-fold, suggesting that mitochondrial respiration could be involved in the pro-oxidant state of Bcl-2-overexpressing cells (Figure 1d). The relationship between mitochondrial O_2^- production and mitochondrial respiration has also been shown in HeLa cells from our previous study[25] (Supplementary Figure S1a, b). To ascertain that our observation was not exclusive to CEM cells, we tested our hypothesis in three other cancer cell lines, namely HK-1 and C666-1 (nasopharyngeal carcinoma) and HCT116 colorectal carcinoma. It is noteworthy that the levels of Bcl-2 expressed in the respective cell lines corresponded with levels of mitochondrial O_2^- (HK-1, 227.5 ± 10.6 relative light units (RLUs)/s per μg protein; C666-1, 17.5 ± 3.54 RLU/s per μg protein; HCT116, 115 ± 49.5 RLU/s per μg protein) and COX activity (HK-1, 1; C666-1, 0.20 ± 0.16; HCT116, 0.24 ± 0.04) (Figure 1e–g). There was no significant difference in citrate synthase activity in all three cell lines (Supplementary Figure S4b). These data provide strong evidence that the effect by Bcl-2 overexpression on mitochondrial respiration and COX activity was not a function of enforced expression, but indeed a true reflection of the effect of Bcl-2 on mitochondrial physiology.

Bcl-2 interacts with the nuclear-encoded subunit Va of COX. Having established the fact that Bcl-2 expression resulted in increased COX activity and mitochondrial respiration, we investigated the possibility of a physical association between Bcl-2 and COX. Using DaliLite Pairwise comparison software (www.ebi.ac.uk/DaliLite/), human Bcl-2 was compared against all subunits of bovine COX enzyme on the basis of structures available from PDB. Of the 13 COX subunits, only COX Va produced a significant *z*-score, suggesting a structural homology between the two proteins (Figure 2a). Despite considerable primary structural differences between bovine and human COX Va, further analysis using BLAST revealed that the region of COX Va bearing a structural homology with Bcl-2 was conserved in both species. Using this information, coimmunoprecipitation studies were performed. A protein–protein interaction was identified between Bcl-2 and COX Va but not with COX Vb (Figure 2b, c, Supplementary Figure S6b). Interaction between COX Va and Bcl-2 seems to be fairly specific, as COX Va did not interact with Bcl-xL, Bax or Bak, members of the Bcl-2 family of proteins (Figure 2d). Using an immunocapture kit (MitoSciences, Eugene, OR, USA) to isolate intact COX, interaction between Bcl-2 and the respiratory enzyme was conclusively demonstrated (Figure 2e). Capitalizing on the distinctly different endogenous Bcl-2 expression in HK-1 and C666-1 cells, coimmunoprecipitation experiments yielded similar results to those from CEM cell lines, suggesting the physical association between Bcl-2 and COX Va but not COX Vb (Figure 2f).

A high Bcl-2 expression leads to an enhanced localization of COX Va to the mitochondria without affecting its expression. To delineate the functional relevance of Bcl-2 interaction with COX Va, isolation of intact mitochondria and subfractionation into its inner mitochondrial fraction were carried out using 20 μg/ml proteinase K to remove the outer mitochondrial membrane. Localization of COX Va in the whole mitochondria and inner mitochondrial fractions was enhanced in CEM/Bcl-2 cells when compared with CEM/Neo cells (Figure 3a, Supplementary Figure S6a). Fractionation of CEM cells into respective subcellular components revealed an increased localization of COX Va in the mitochondria over the nuclear fraction in CEM/Bcl-2 cells (Figure 3a). The reverse was observed in CEM/Neo cells (Figure 3a). Differences in the localization of COX Va observed by western blot analysis were correspondingly quantified by densitometry analysis (Figure 3a). Serendipitously, overexpression of Bcl-2 also resulted in an improved localization of COX Vb into the inner mitochondria of these cells (Figure 3a). An increased localization of COX Vb into the inner mitochondria may have an unprecedented role in regulating COX activity, thus contributing to a pro-oxidant state in CEM/Bcl-2 cells during

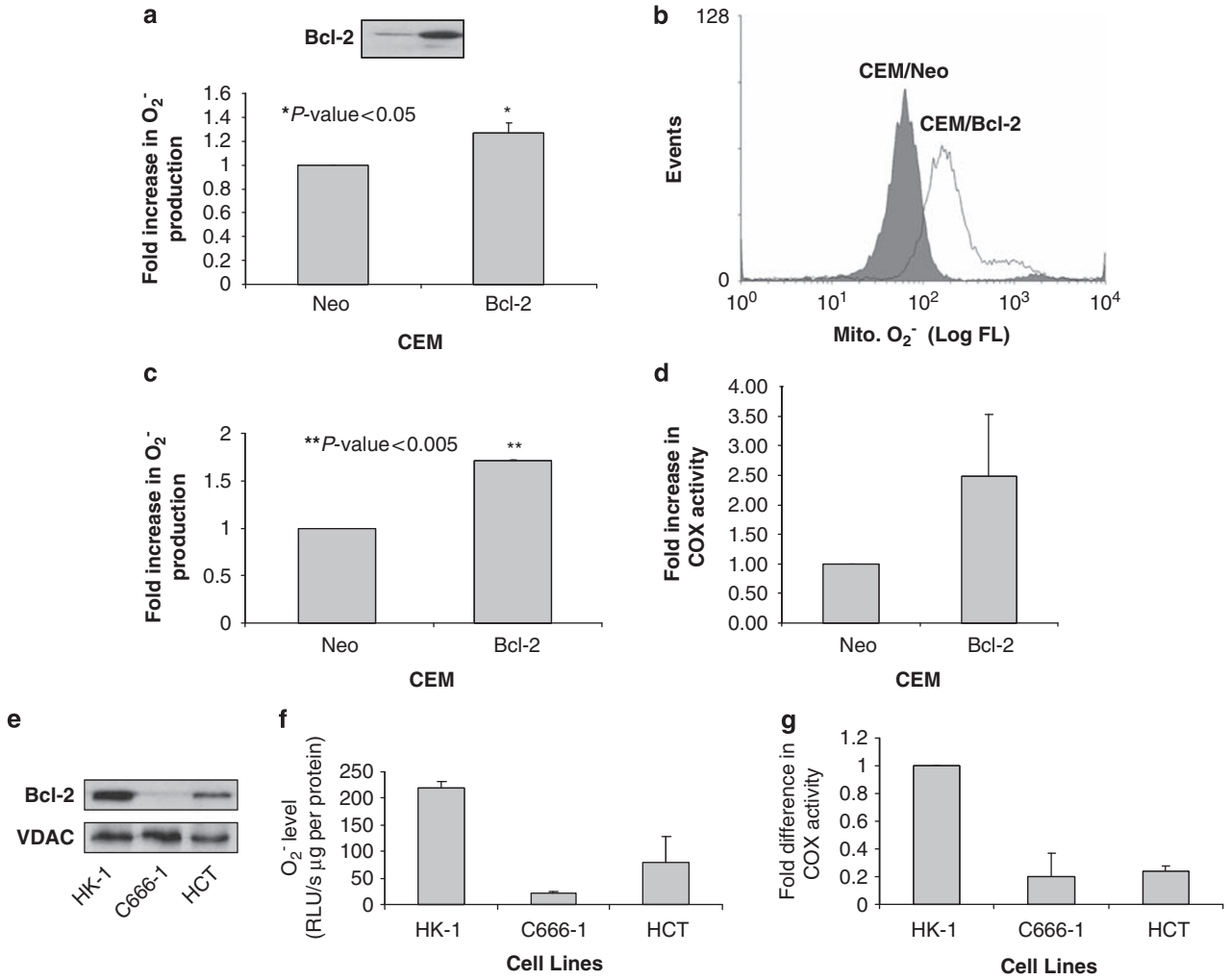

Figure 1 CEM cells overexpressing Bcl-2 have higher levels of O_2^- and COX activity. (**a**) Using lucigenin-based chemiluminescence assay, intracellular O_2^- production was quantified in CEM/Neo and CEM/Bcl-2 cells. Overexpression of Bcl-2 is evident from western blot analysis. (**b**) Using MitoSOX Red probe, mitochondrial O_2^- was determined by flow cytometry. (**c**) Mitochondrial O_2^- from CEM/Neo and CEM/Bcl-2 cells was similarly measured as in panel **a**. (**d**) COX activity in both cells lines was determined spectrophotometrically using reduced cytochrome *c*. (**e**) Expression of mitochondrial-localized Bcl-2 was determined in HK-1, C666-1 and HCT116116 cell lines. VDAC was probed as a mitochondrial control marker. (**f**, **g**) Corresponding levels of mitochondrial O_2^- and COX activity were assayed in HK-1, C666-1 and HCT116 cell lines. The error bars in panels **a**, **c**, **d**, **f** and **g** represent the mean ± S.D. ($n = 3$)

normal conditions. More importantly, Bcl-2 overexpression-mediated COX activity was not a function of changing COX Va and Vb expression but that of improved targeting of nuclear-encoded mitochondrial proteins (Figure 3a, Supplementary Figure S6a).

To verify our mitochondrial isolation technique, we repeated the experiment this time using an established protocol for the isolation of mitochondria.[26] Again, COX Va was more prominently localized to the mitochondria of Bcl-2-overexpressing CEM cells (Supplementary Figure S2a). Furthermore, to ensure that our mitochondrial fractions were free from cytosolic contamination, we loaded increasing amounts of mitochondrial proteins and did not detect a corresponding increase in CuZn SOD, a faithful cytosolic protein marker, compared with COX Va and prohibitin (Supplementary Figure S2b).

Transient overexpression and knockdown of Bcl-2 by siRNA were performed to investigate whether the phenomenon observed in CEM/Neo and CEM/Bcl-2 cells could be reversed. Indeed, the overexpression of Bcl-2 in CEM cells increased the localization of COX Va from the nucleus to the mitochondria and the silencing of Bcl-2 in CEM/Bcl-2 cells reversed the effect (Figure 3b). Repeating earlier experiments using HK-1 and C666-1 cells with inherently contrasting levels of Bcl-2 expression corroborated our previous findings with CEM cells (Figure 3c). Similarly, Bcl-2 silencing with siRNA reverted the observations in HK-1 cells to that akin to C666-1 cells (Figure 3d). Further reinforcing the role of Bcl-2 in promoting the localization of COX Va to the mitochondria in transformed cells, lymphoma samples from three different patients reaffirmed this aspect of Bcl-2 (Figure 3e).

In addition, immunofluorescence confocal microscopy showed the colocalization of COX Va and Bcl-2 (Figure 3f). Furthermore, an overexpression of Bcl-2 correlated with the intracellular localization of COX Va in a concentrated manner as opposed to the dispersed localization of COX Va in

a

PDB code / chain	Protein	*Z*-score	Aligned residues
1GJH / A	Bcl-2	3.5	65
1V54 / E	COX Va		
1GJH / A	Bcl-2	Nil	Nil
1V54 / F	COX Vb		

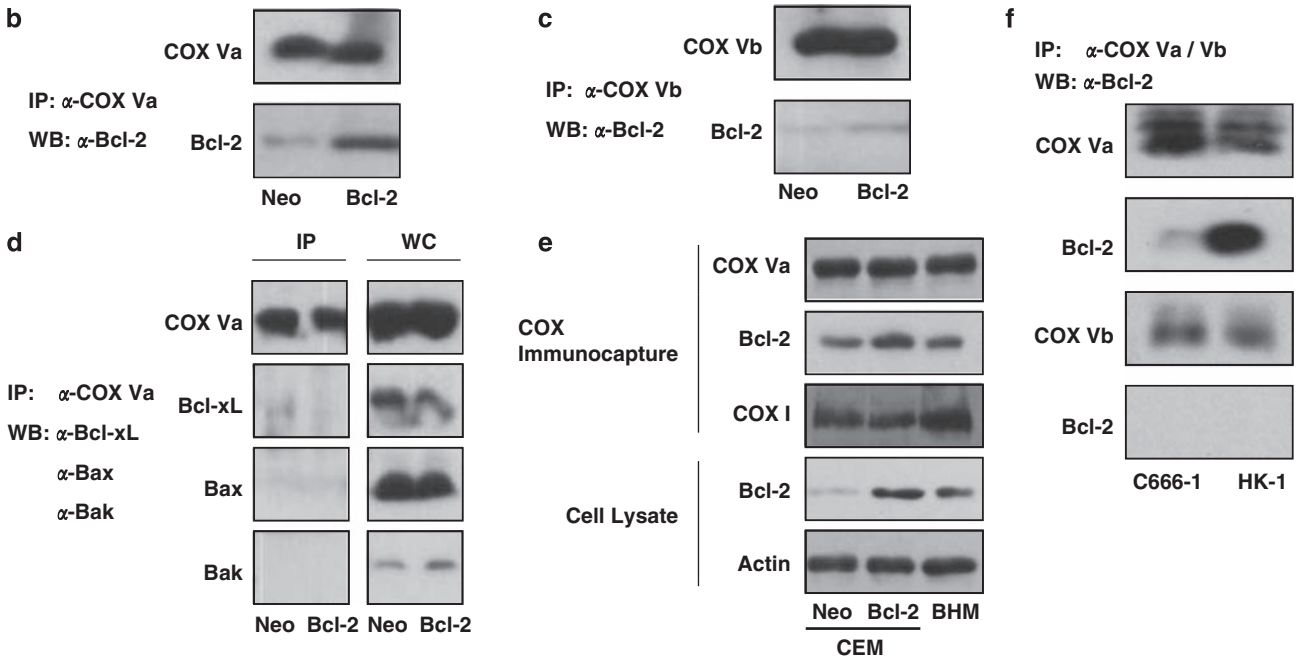

Figure 2 Bcl-2 interacts with subunit Va of the COX enzyme. (**a**) Using DaliLite Pairwise comparison software and protein structures from PDB, human Bcl-2 scored the only significant hit with bovine COX Va, indicative of structural homology and a possible interaction between the two proteins. *z*-score >2 is considered significant. (**b**, **c**) By means of coimmunoprecipitation, Bcl-2 interaction with COX Va and its nonassociation with COX Vb were affirmed in CEM/Neo and CEM/Bcl-2 cells. (**d**) Furthermore, COX Va did not interact with Bcl-xL, Bax and Bak, which are all proteins of the Bcl-2 family with conserved domains. Coimmunoprecipitation was performed with 0.8 mg protein in each sample. (**e**) Association of Bcl-2 with the COX enzyme was confirmed by the COX immunocapture kit from MitoSciences. Isolation of intact COX was performed as recommended by the vendor. Bovine heart mitochondria sample (BHM) was supplied by MitoSciences as a positive control. COX I was probed as a control marker for the presence of COX, and actin was probed as a loading control for whole-cell lysate. (**f**) Coimmunoprecipitation experiments repeated as before on HK-1 and C666-1 cells using COX Va and Vb as the respective bait proteins demonstrated a protein–protein interaction between Bcl-2 and COX Va, but not Vb

nontransfected cells (Figure 3f). Confocal microscopy imaging provided evidence indicating significantly higher COX Va localization to the mitochondria of CEM/Bcl-2 cells compared with CEM/Neo cells (Figure3g).

Taken together, these results reiterate the functional relevance of Bcl-2 interaction with COX Va in terms of promoting COX Va incorporation into the mitochondria. It is plausible that overexpression of Bcl-2 might increase COX activity by improving COX Va distribution to mitochondria without affecting its expression.

Bcl-2 modulates mitochondrial respiration during stress states by stabilizing COX Va and decreasing COX Vb in the mitochondria. To further our understanding of the regulatory role of Bcl-2 in mitochondrial respiration and COX activity for the maintenance of redox status in the face of oxidative insults, we subjected CEM/Neo and Bcl-2 cells to physiological stress states aimed at the early induction of oxidative insult. Induction of mitochondrial oxidative stress by 5 μg/ml antimycin for 1 h did not alter the global expression of COX Va and Vb (Figure 4a). Interestingly, western blot analysis of isolated inner mitochondria from CEM/Bcl-2 cells treated similarly indicated a slight upregulation of COX Va and a downregulation of COX Vb (Figure 4b). The reverse was observed in CEM/Neo cells (Figure 4b). A combined treatment for 1 h with 20 ng/ml leptomycin B, a nuclear export inhibitor, did not affect the respective observations, but exacerbated the antimycin-treated conditions, suggesting that the nuclear export machinery may not be responsible for the alterations in the targeting of COX subunits to the mitochondria on oxidative stress in CEM cells. Next, CEM/Neo and Bcl-2 cells were subjected to serum deprivation in a dose-dependent manner for 24 h. From 5 to 0.5% serum, isolated inner mitochondria from CEM/Bcl-2 cells showed a sustained presence of COX Va and a gradual removal of COX Vb, whereas CEM/Neo samples stabilized COX Vb and degraded COX Va (Figure 4c). The expression level of these proteins in both cell lines remained comparable in the nuclear fractions, although 0.5% serum seemingly increased the COX Vb expression in CEM/Neo cells (Figure 4c).

CEM/Neo and Bcl-2 cells were subjected to various oxidative stress-inducing conditions that included glucose withdrawal and hypoxia. All three conditions maintained over 3 h resulted in the stabilization of COX Va and in the downregulation of COX Vb in the isolated inner mitochondria of CEM/Bcl-2 cells and vice versa in CEM/Neo samples, although to a varying extent (Figure 4d).

Mitochondrial oxidative stress stimulates Bcl-2-overexpressing tumor cells to downregulate COX activity, maintaining mitochondrial redox status, transmembrane potential and ATP levels. Indeed, induction of hypoxia for 10 min, as well as glucose deprivation or serum deprivation for 30 min, was sufficient to induce early mitochondrial oxidative burst in the form of O_2^- in both CEM cell lines (Neo: ~1.8- to 2.6-fold, Bcl-2: ~1.7- to 2.0-fold) (Figure 5a, Supplementary Figure S3a). In terms of functionality, a subsequent maintenance of the respective stress conditions over 3 h resulted in a further increase in mitochondrial O_2^- in CEM/Neo cells by ~1.9- to 4.5-fold,

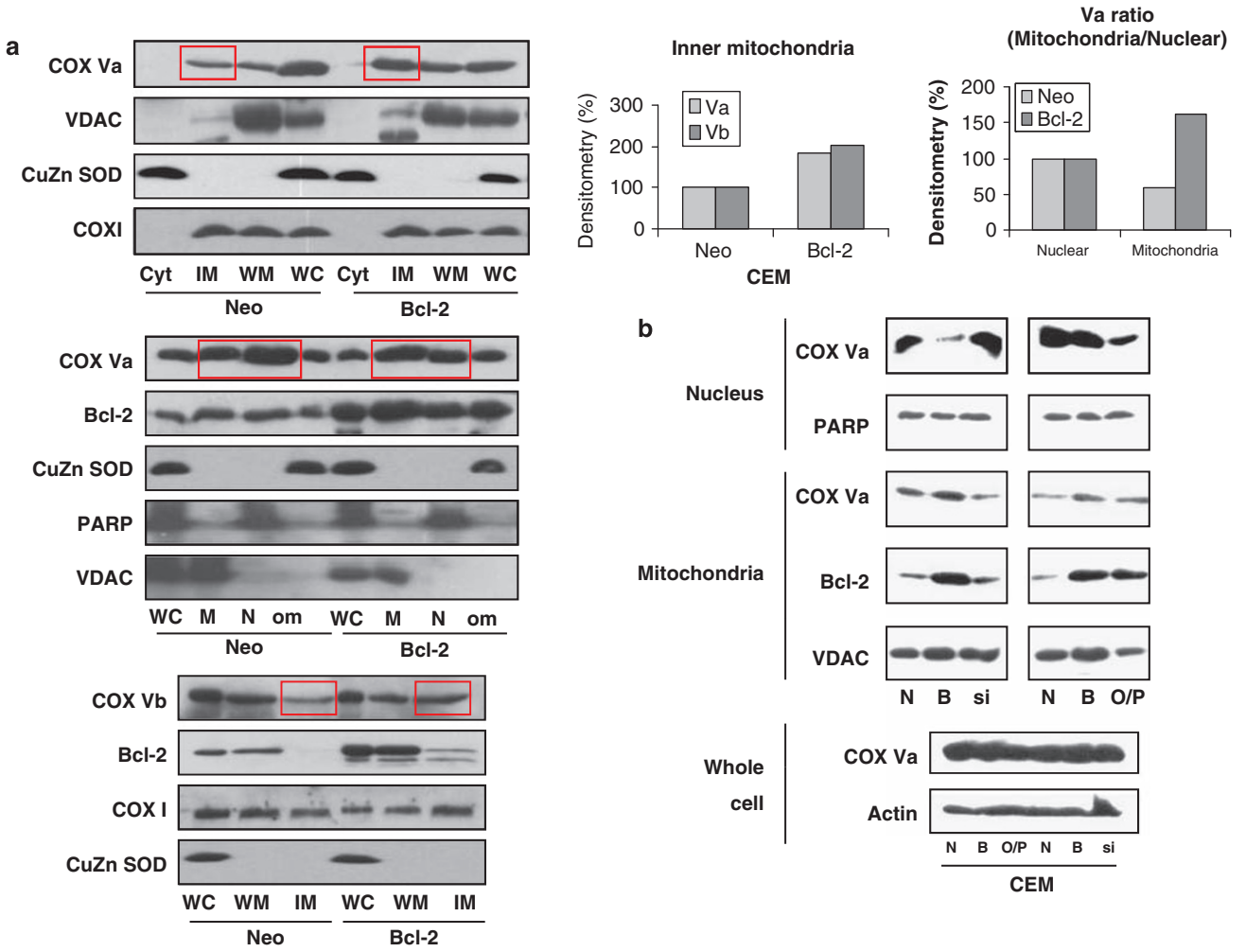

Figure 3 Bcl-2 expression promotes COX Va localization to the mitochondria. (**a**) The presence of COX Va and Vb in various subcellular compartments was determined in CEM/Neo and CEM/Bcl-2 cells. The respective abbreviations contain the following annotations: IM – inner mitochondria, WM – whole mitochondria, WC – whole cell, M – mitochondria, N – nuclear, Cyt – cytosol, om – other membranes. Densitometry analysis of the various bands highlighted in red is represented graphically. The presence of VDAC and Bcl-2, COX I, CuZn SOD and PARP represented whole mitochondria/outer mitochondrial membrane, inner mitochondrial membrane, cytosolic and nuclear compartments, respectively. (**b**) Effects of Bcl-2 overexpression in CEM/Neo and knockdown in CEM/Bcl-2 cells on COX Va mitochondrial and nuclear localization. Bcl-2 overexpression and silencing were detected 48 h and 72 h after transfection, respectively. The respective abbreviations contain the following annotations: N – CEM/Neo, B – CEM/Bcl-2, O/P – overexpression, si – silencing. The total expression of COX Va remained unaffected. PARP, VDAC and actin were probed as control markers for nucleus, mitochondria and whole-cell lysate, respectively. (**c**) The detection of COX Va and Vb in various mitochondrial fractions was repeated as before on HK-1 and C666-1 cells. The respective abbreviations contain the following annotations: IM – inner mitochondria, WM – whole mitochondria, WC – whole cell. COX I and VDAC were probed as control markers for inner mitochondria and whole mitochondria, respectively. (**d**) The evaluation of COX Va and Vb mitochondrial localization in HK-1 cells after Bcl-2 knockdown with siRNA. The respective abbreviations contain the following annotations: IM – inner mitochondria, WM – whole mitochondria, WC – whole cell. COX I, VDAC and actin were probed as control markers for inner mitochondria, whole mitochondria and whole-cell lysate, respectively. (**e**) Using lymphoma cells from three patient samples, the extent of COX Va localization to the mitochondria was assessed in relation to the respective levels of Bcl-2 expression. VDAC and actin were probed as loading control markers for mitochondria and whole-cell lysate, respectively. (**f**) Overexpression of Bcl-2, Bcl-2 colocalization with COX Va and COX Va localization patterns were demonstrated using confocal microscopy. (**g**) Mitochondrial localization of COX Va in CEM/Neo and CEM/Bcl-2 cells was determined by confocal microscopy. Duplicates were performed for CEM/Neo cells in panels **f** and **g**

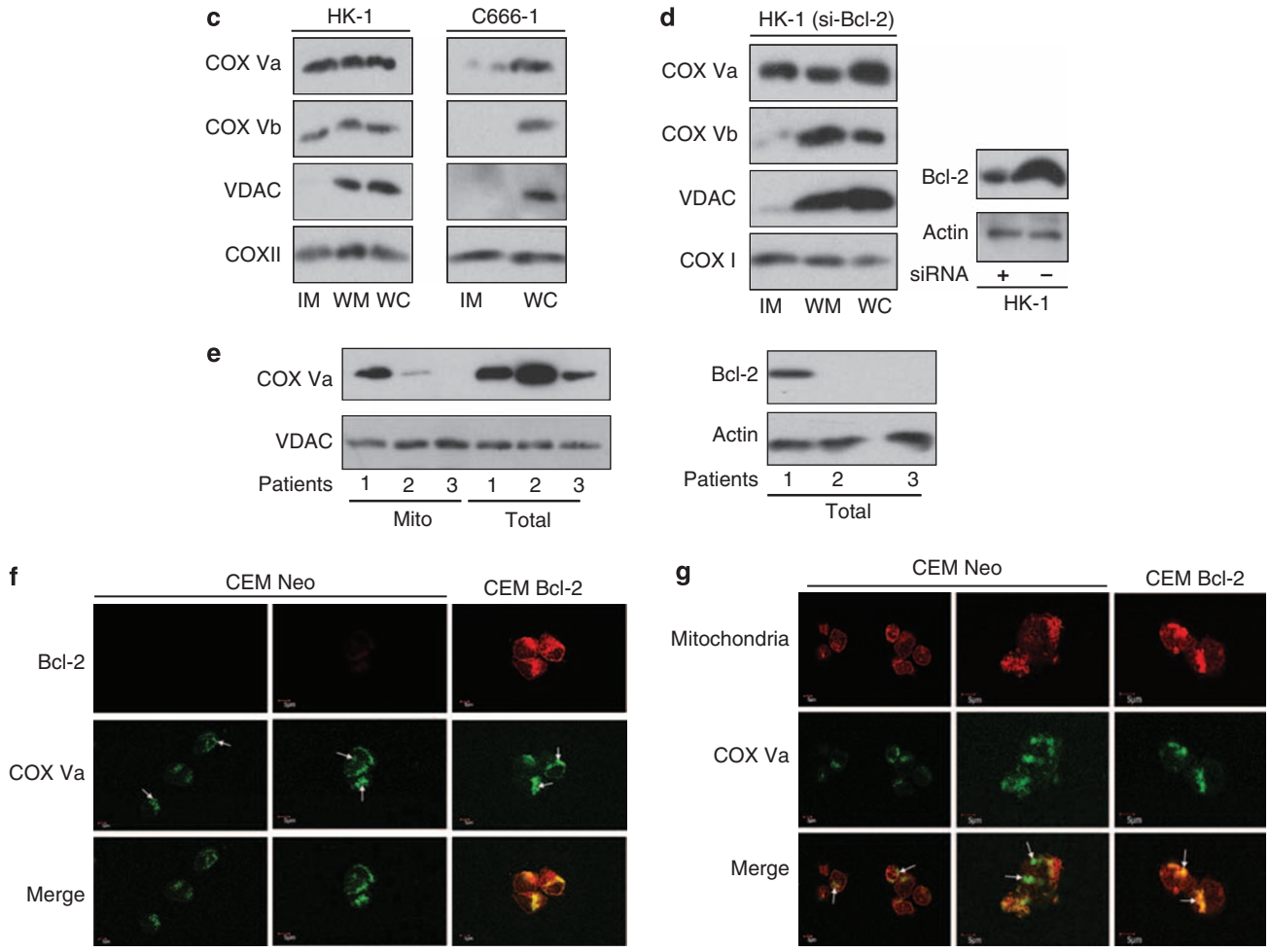

Figure 3 Continued.

whereas the levels of the species were stabilized in their CEM/Bcl-2 counterparts, which could be a function of the downregulation in COX activity (>50%) and vice versa in CEM/Neo cells, suggesting that fluctuations in COX Va and Vb distribution within the mitochondria might have a role in defining the level of COX activity (Figure 5b, c, Supplementary Figure S3b, c). In addition, hypoxia, serum withdrawal and glucose deprivation did not alter the transmembrane potential and mitochondrial ATP production in CEM/Bcl-2 cells (Figure 5d, e). In contrast, all three conditions resulted in a depolarization of the transmembrane potential and in slight increases in mitochondrial ATP production in CEM/Neo cells (Figure 5d, e). However, untreated and treated CEM/Bcl-2 cells consistently produced more mitochondrial ATP than did CEM/Neo under all conditions (Figure 5e). The basal mitochondrial transmembrane potential was also slightly higher in CEM/Bcl-2 cells than in CEM/Neo cells (Figure 5d). Moreover, the effect on COX exerted by these physiological stress conditions did not involve complex I, II, III and citrate synthase (Supplementary Figure S4a, b).

Bcl-2 interaction with COX Va is predominantly mediated by the BH2 domain and C-terminal region of Bcl-2. Finally, we sought to address the interacting domains of Bcl-2 with COX Va. On the basis of DaliLite Pairwise comparison software and using site-directed mutagenesis, we generated a BH4 domain mutant (R26K), a C-terminal region mutant (A234G) and a BH2 domain mutant harboring a single mutation at the BH2 domain and multiple mutations at its flanking upstream and downstream regions (Figure 6a). The protein–protein interaction between Bcl-2 and COX Va was significantly reduced in CEM/Neo cells overexpressing the BH2 domain mutant (Figure 6b). Similarly, the C-terminal region mutant showed a slightly reduced association with COX Va (Figure 6b). In contrast, mutation at the BH4 domain failed to disrupt Bcl-2 binding to COX Va on the basis of coimmunoprecipitation studies (Figure 6b). A reduced interaction between C-terminal and BH2 mutants with COX Va resulted in a corresponding decrease in the mitochondrial localization of COX Va and COX activity to the basal levels of CEM/Neo cells, which, in turn, exerted a likely consequential effect on the by-production of O_2^- through decreased mitochondrial respiration, affecting the overall redox status in these cells (Figure 6b–d). In contrast, the overexpression of Bcl-2 mutated at the BH4 domain in CEM/Neo cells restored COX Va mitochondrial localization, COX activity and the

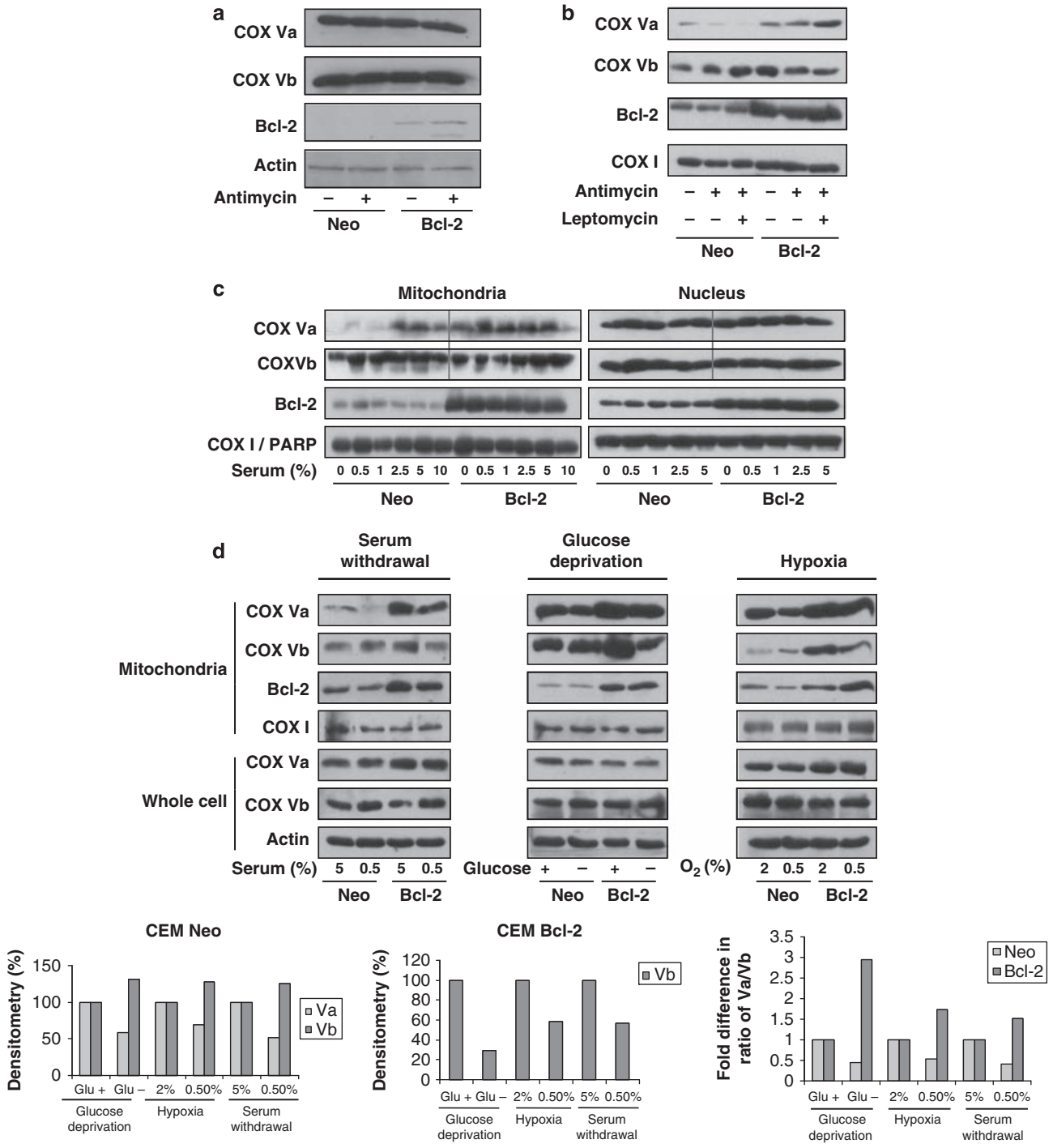

Figure 4 Bcl-2 has a role in tumor metabolic adaptation during stress conditions by altering mitochondrial levels of COX Va and Vb. (**a**) Total COX Va and Vb expression was unaffected after treatment with 5 μg/ml antimycin for 1 h. (**b**) Mitochondrial levels of COX Va and Vb were altered on antimycin treatment alone and in combination with 20 ng/ml leptomycin B for 1 h. (**c**) Levels of COX Va and Vb in the mitochondrial and nuclear compartments of CEM/Neo and CEM/Bcl-2 cells respond to 24 h of serum deprivation in a dose-dependent manner, although differently in both cell lines. (**d**) Mitochondrial and whole-cell expression of COX Va and Vb was assessed in CEM/Neo and CEM/Bcl-2 cells on induction of serum withdrawal, glucose deprivation and hypoxia for 3 h. Densitometry analysis of the changing levels and ratio of COX Va and Vb in both cell lines during these stress conditions are represented graphically. Bcl-2 was separately probed using whole mitochondria to detect for overexpression before the outer mitochondrial membrane was removed. Actin, COX I and PARP were probed as control markers for whole-cell lysate, inner mitochondria and nucleus, respectively, in panels **a**–**d**

corresponding O_2^- levels to that of CEM/Bcl-2 cells, suggesting the noninvolvement of the BH4 domain in this unique role of Bcl-2 in regulating mitochondrial respiration through COX activity (Figure 6b–d). There was no considerable difference in citrate synthase activity to confound our COX activity measurements (Supplementary Figure S4b).

Discussion

In this study, we showed that Bcl-2-mediated increase in COX activity is due to the enhanced presence of COX Va and Vb in the mitochondria, indicative of a more complete and stable COX enzyme. Our results showed that an increase in mitochondrial Bcl-2 as a result of an intrinsic high expression or overexpression directly promotes the translocation of nuclear-encoded COX Va to the mitochondria through a physical interaction, without affecting its expression. The increased presence of mitochondrial COX Va is not due to an increase in the formation of the initial COX intermediate, as the level of mitochondrial-encoded COX I has been shown to be unaffected in Bcl-2-overexpressing tumor cells previously.[25] Indeed, using COX I as a marker, one-dimensional BN-PAGE revealed more partially assembled COX subcomplexes in CEM/Neo compared with CEM/Bcl-2 cells, further confirming the lower amounts of mitochondrial COX Va in cells with a lower Bcl-2 expression (Supplementary Figure S5). Furthermore, taking into consideration the fact that both Bcl-2 and COX Va are nuclear-encoded, mitochondria-targeted

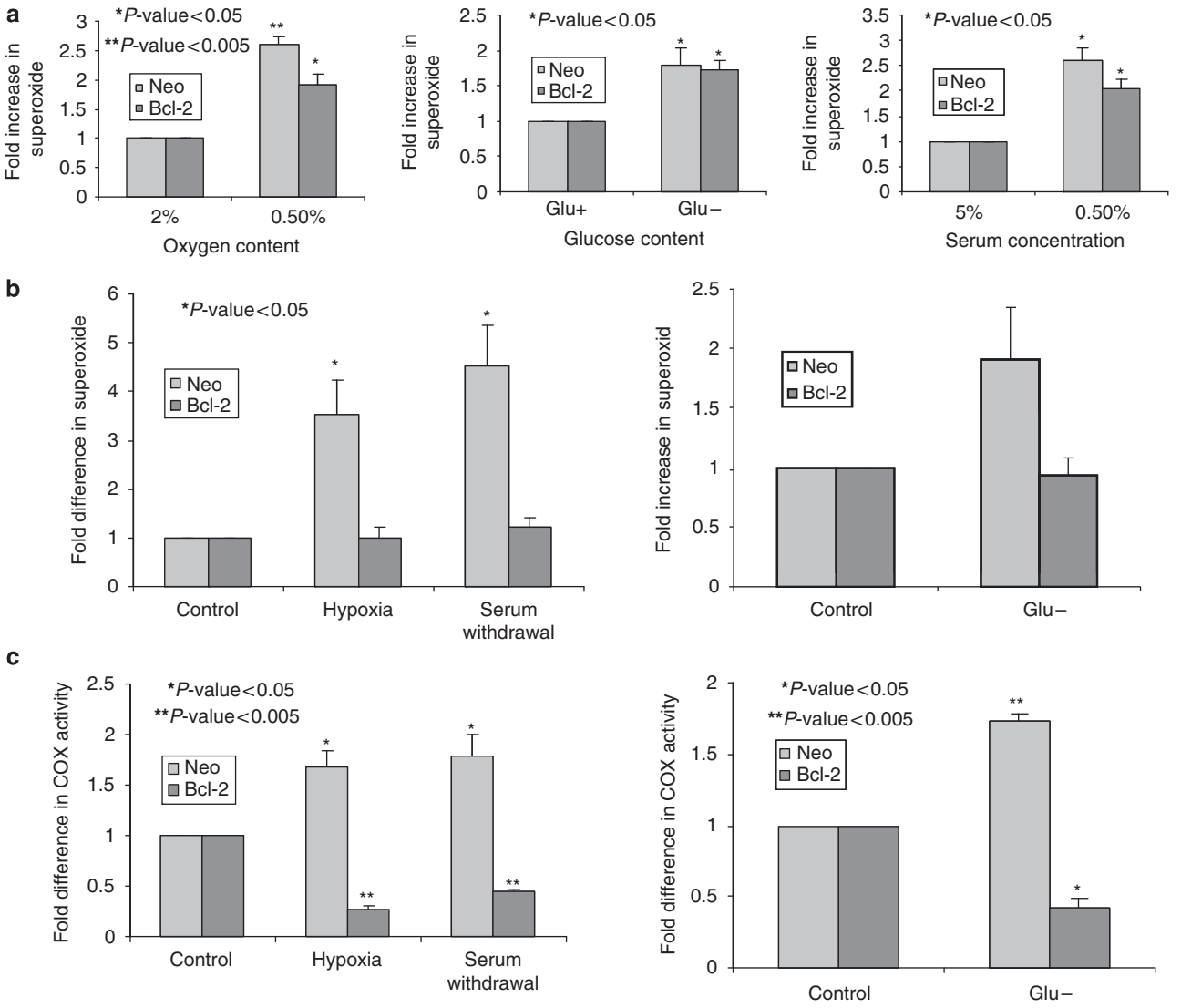

Figure 5 CEM/Bcl-2 cells are able to downregulate mitochondrial respiration and maintain mitochondrial O_2^- levels in response to an early burst of ROS induced by stress conditions. (**a**) The initial induction of mitochondrial O_2^- production in CEM/Neo and CEM/Bcl-2 cells after exposure to hypoxia for 10 min or glucose deprivation or serum withdrawal for 30 min. (**b**) Mitochondrial O_2^- production in CEM/Neo and CEM/Bcl-2 cells after exposure to 3 h of respective stress conditions, measured using lucigenin-based chemiluminescence assay carried out on isolated mitochondria. (**c**) The corresponding COX activity in both cell lines was measured in response to the various oxidative stress-inducing conditions after 3 h of exposure. (**d**) Mitochondrial transmembrane potential was assessed in both cell lines at basal and stress conditions. (**e**) Mitochondrial ATP production was also quantified with fold differences normalized with respect to CEM/Neo under normal conditions. The error bars in panels **a**–**c** and **e** represent the mean ± S.D. ($n = 3$)

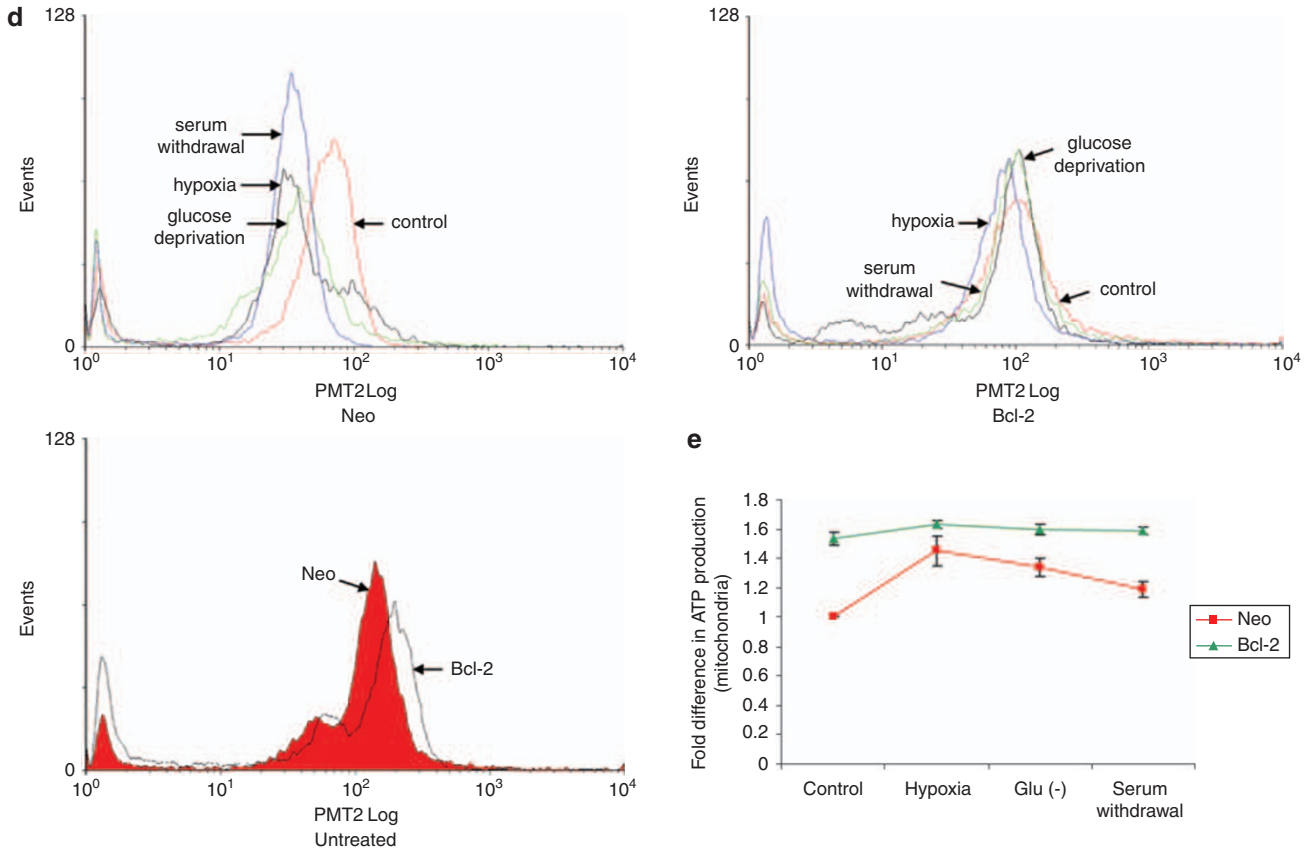

Figure 5 Continued

proteins, we propose Bcl-2 as a likely chaperone to COX Va, facilitating its targeting to the mitochondria, resulting in a more inclusive COX, capable of greater enzymatic activity. On the other hand, an increased COX Vb presence in the inner mitochondrial membrane, despite no physical association with Bcl-2, could be a collateral effect of Bcl-2 insertion at the outer mitochondrial membrane and a subsequent alteration of membrane dynamics, allowing more COX Vb to traverse across membranes. Furthermore, the yeast analog of COX Vb, COX IV, has been shown to be post-transcriptionally regulated by the cardiolipin content of the mitochondria.[27] The likelihood of Bcl-2 affecting COX Vb localization to the outer mitochondrial membrane is ruled out, as total COX Vb from the intact mitochondria fraction is the same in CEM/Neo and Bcl-2 cells, suggesting that Bcl-2-mediated COX Vb translocation across mitochondrial membranes may be linked to the enhanced localization of COX Va. One possible explanation would be that COX assembly is a multistep process and COX Va is upstream of COX Vb in the assembly hierarchy; increased COX Va-assembled intermediates may promote the downstream incorporation of COX Vb, which has been harboring at the outer mitochondrial membrane, waiting for translocation into the inner mitochondrial membrane to form COX. Alternatively, Bcl-2 and the yeast homolog COX IV (COX Vb) have also been shown to interact with mitochondrial import protein Tom20 in *Saccharomyces cerevisiae*, an implication that Bcl-2 may similarly promote the import of COX Vb across mitochondrial membranes through Tom20 in the mammalian system.[28,29]

Increased COX Va and Vb in the inner mitochondrial compartment of high Bcl-2-expressing tumor cells reflects the greater capacity of these cells to carry out oxidative phosphorylation and mitochondrial respiration, encouraging ATP production. In parallel, by-production of O_2^- is augmented, resulting in the pro-oxidant state reported in tumor cells with a high Bcl-2 expression[20,25] (Figure 7a). Our study suggests that despite tumor cells preferentially utilizing glycolysis instead of oxidative phosphorylation as the primary source of energy production as postulated by Warburg, anti-apoptotic proteins such as Bcl-2 may exert dual functions in its protective role: the first is the canonical inhibition of pro-apoptotic proteins and the safeguard of mitochondrial membrane integrity to prevent the execution of apoptosis; the second is the nonclassical optimization of mitochondrial respiration and the prevention of the excessive compromise of mitochondrial respiration in tumor cells to boost ATP production and a level of ROS most suited for pro-survival signaling. Indeed, this novel function of Bcl-2 seems to be dependent on its BH2 domain, the mutation of which affects its binding to Bax without affecting its homodimerization, accounting for the death-repressive activity of Bcl-2.[30] This may explain the dominant-negative effect of BH2-mutated Bcl-2 on COX activity over nontransfected control. The overexpression of mutant BH2-Bcl-2, in addition to its ability to inhibit the

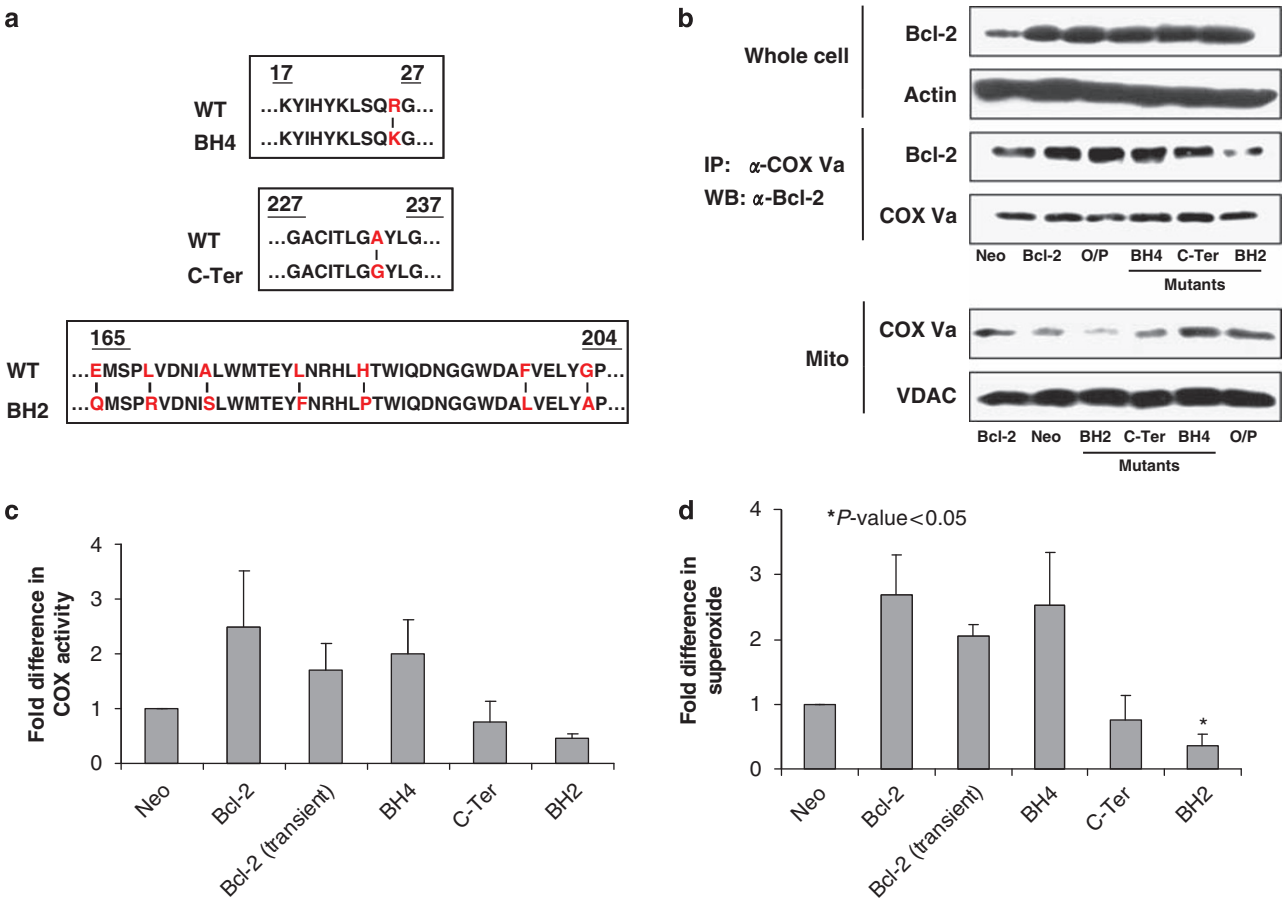

Figure 6 Involvement of the BH2 domain and its flanking regions, as well as the C-terminal region of Bcl-2, in mediating interaction with COX Va. (**a**) Generation of various Bcl-2 mutants and their respective mutated amino-acid positions. (**b**) Coimmunoprecipitation between stably transfected empty vector (Neo), stably transfected wild-type Bcl-2, transiently transfected (O/P) wild-type Bcl-2 and the respective transiently transfected Bcl-2 mutants with COX Va in CEM cells. The level of COX Va localization to mitochondria was subsequently analyzed in these various samples. Actin and VDAC were probed as control markers for whole-cell lysate and mitochondria, respectively. (**c**, **d**) COX activity and mitochondrial O_2^- were correspondingly assessed on the basis of the samples in panel **b**. The error bars in panels **c** and **d** represent the mean ± S.D. ($n = 3$)

interaction between COX Va and Bcl-2, may also homodimerize (with the resident Bcl-2) and neutralize any COX Va-binding ability of basal Bcl-2. In the absence of Bcl-2, tumor cells rely predominantly on glycolysis for energy and inhibit mitochondrial functions to a level below that of normal cells to prevent the onset of the death programme. Thus, it is conceivable that cancer cells may seek to preserve their mitochondrial functions through this novel role of anti-apoptotic Bcl-2 to increase the chances of survival and invasion.

The ability of Bcl-2 to fine-tune COX activity by adjusting the distribution of COX Va and Vb in the mitochondria throughout different stress conditions reflects the importance of the composition of subunits in COX during metabolic reprogramming for cancer cells (Figure 7a). Many studies have established the expression of yeast homologs COX IV and VI (COX Vb and Va) as being aerobically regulated, whereby the expression is positively correlated to the oxygen content.[5–8] Furthermore, yeast COX VI is repressed by glucose.[31,32] In this respect, our results indicate that regulation of COX subunits during metabolic adaptation may be controlled by oncoproteins such as Bcl-2. During hypoxia, overexpression of Bcl-2 stabilized COX Va and reduced the COX Vb mitochondrial presence, whereas the reverse was detected in the absence of Bcl-2 overexpression. These cells responded similarly under a glucose-deprived condition. In light of this, we demonstrated for the first time that adaptations in tumor metabolism are intrinsically different from physiological adaptations in the yeast model in response to oxygen and glucose tensions, further distinguished by the ability of Bcl-2 to alter the responses of COX Va to oxygen and glucose.

In addition, our results suggest that during oxidative stress, COX Vb may replace COX Va in increasing COX activity, whereas COX Va may have a regulatory role in keeping COX activity in check. This is evident from our observation that on oxidative stress, lack of COX Va in the presence of COX Vb resulted in a significant upregulation of COX activity in CEM/Neo cells, whereas the stable presence of COX Va in the absence of COX Vb resulted in the downregulation of COX activity in CEM/Bcl-2 cells. This is in addition to the role that COX Va has during normal conditions in which increased mitochondrial COX Va leads to higher COX activity. Collectively, these results suggest that COX subunits may exhibit interchangeable roles to determine COX activity, depending on the microenvironment of tumor cells; and Bcl-2 may be central to this regulation (Figure 7a, b). Our study highlights

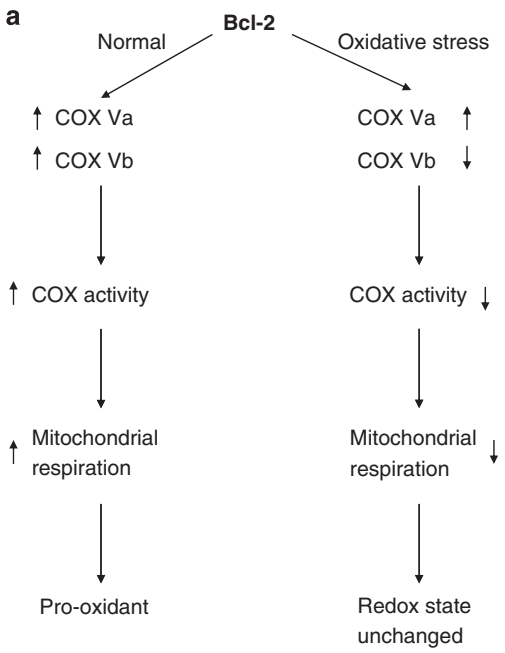

b

Conditions / Subunits	Normal	Oxidative stress
COX Va	Increases COX activity	Regulates COX activity
COX Vb	-	Increases COX activity

Figure 7 Schematic diagram highlighting the central role of Bcl-2 and COX subunits in tumor mitochondrial respiration regulation. (**a**) Bcl-2 regulation of mitochondrial respiration and the redox state through adjustment of COX subunits. (**b**) Roles that COX Va and Vb have under normal and oxidative stress conditions

the importance of the regulation behind the incorporation of these subunits to form COX and the resultant impact on COX activity during basal tumor metabolism and adjustments to oxidative stress.

Downregulation of mitochondrial respiration and maintenance of mitochondrial O_2^- production in the face of potentially deleterious conditions reflect the plasticity of tumor metabolism, fine-tuned by Bcl-2 with respect to COX. Cancer cells are often saddled with various stress conditions, and this may reflect a novel function of Bcl-2 in aiding these cells to overcome the treacherous barriers faced during metastasis, while maintaining the redox milieu and energy production necessary for survival. A more important implication in terms of cancer therapeutics could suggest that certain tumors with an intrinsically high Bcl-2 expression may render them more refractory to ROS-based treatments compared with other tumors with a low basal Bcl-2 expression, corresponding to better prognosis. In this study, we provide an additional mechanism to Bcl-2-induced chemoresistance through the mitochondrial respiratory pathway, as well as reiterate the importance of Bcl-2-targeted therapies and the significance of COX Va and Vb as cancer markers.

Materials and Methods

Cell culture. CEM human leukemia cells stably transfected with the control vector (CEM/Neo) or Bcl-2 (CEM/Bcl-2) were maintained in RPMI 1640 supplemented with 2 mM L-glutamine, 1% streptomycin–penicillin (v/v) and 5% FBS (v/v). G418 disulfate salt solution was added as a selective antibiotic for the maintenance of stable transfectants. HK-1 and C666-1 cell lines were derived from nasopharyngeal carcinoma, which was maintained in RPMI 1640 supplemented with the constituent mentioned previously and 10% FBS (v/v), without G418 antibiotic. HCT116 is a colon carcinoma cell line maintained in McCoy's 5A medium similarly supplemented as that for HK-1 and C666-1. All cell lines were cultured in a humidified incubator at 37°C and 5% CO_2.

Isolation of nuclear fraction. Cells were harvested and washed with ice-cold 1 × PBS and spun down by centrifugation at 1500 × *g* for 3 min at 4°C. The resultant pellets were resuspended in 400 μl Buffer A (10 mM HEPES, 10 mM KCL, 0.1 mM EDTA and 0.1 mM EGTA at pH 7.9) and were left to swell for 15 min on ice. Thereafter, 25 μl of 10% NP-40 was added before vortexing for 10 s. The insoluble nuclear fraction was collected by centrifugation at 14 000 r.p.m. for 30 s at 4°C. The nuclear fraction pellet was further resuspended in 50 μl Buffer C (20 mM HEPES, 0.4 mM NaCl, 1 mM EDTA and 1 mM EGTA at pH 7.9) and rocked vigorously for 15 min at 4°C. The resultant supernatant containing the nuclear proteins is obtained by centrifugation at 14000 r.p.m. for 5 min at 4°C.

Measurement of mitochondrial ATP. To inhibit glycolytic ATP production, cells were precultured in medium supplemented with 2-deoxy-glucose and 2 mM pyruvate in place of normal glucose on an equimolar basis, before being subjected to various stress conditions. The level of ATP was quantified using the ATP bioluminescent somatic cell assay kit (Sigma-Aldrich, St. Louis, MO, USA) and was carried out according to instructions from the manufacturer.

Isolation of intact mitochondria. Cells were harvested and washed once with ice-cold 1 × PBS and spun down by centrifugation at 1200 r.p.m. for 5 min at 4°C. The pellet was resuspended in 10 volumes of extraction buffer (200 mM mannitol, 68 mM sucrose, 50 mM Pipes-KOH pH 7.4, 50 mM KCL, 5 mM EGTA, 2 mM $MgCl_2$, 1 mM DTT) containing various protease inhibitors (1 mM PMSF, 10 μg/ml aprotinin, 20 μg/ml pepstatin A and 10 μg/ml leupeptin) and incubated on ice for 20 min. After incubation, the cells were homogenized with a dounce homogenizer and passaged for 30 strokes before being centrifuged at 2000 g for 3 min at 4°C. Thereafter, the supernatant was centrifuged again at 13000 g for 10 min at 4°C as described elsewhere.[33] The pellet contains the intact mitochondria fraction. To obtain mitochondria devoid of the outer mitochondrial membrane, purified mitochondria were treated with 20 μg/ml proteinase K for 25 min on ice. Phenylmethylsulfonyl fluoride was then added to a final concentration of 2 mM and the samples were further incubated for another 10 min on ice as described elsewhere.[33,34] The samples were subjected to centrifugation as described before to obtain isolated mitochondria. A second protocol for the isolation of mitochondria was also performed as described previously to validate our results obtained from the first technique.[26]

Complex I, II, II-III and citrate synthase activity measurements. Complex I activity was determined using the Complex I

Enzyme Activity Microplate Assay Kit (MitoSciences) on the basis of recommended protocol and settings described by the manufacturer. Complex II and II-III activity was quantified on the basis of established protocols described in previous studies.[35,36] Citrate synthase activity was measured using the citrate synthase assay kit (Sigma-Aldrich) and was carried out according to instructions from the vendor.

COX isolation and activity. Cells were dissolved in 2 ml of COX buffer (250 mM sucrose, 2 mM HEPES and 0.1 mM EGTA at pH 7.4) before being centrifuged at 330 $\times$ *g* for 10 min at 4°C. The cells were then resuspended with 1 ml of COX buffer and incubated for 10 min at 4°C before being subjected to homogenization for 10 passages; thereafter, the cell lysate was spun at 600 $\times$ *g* for 10 min at 4°C. The supernatant was then centrifuged at 14 400 $\times$ *g* for 10 min at 4°C. The resultant pellet is the purified mitochondria fraction, containing COX. The pellet was dissolved in 100 μl of prewarmed potassium phosphate buffer at pH 7.2 and was incubated at RT for 3 min. COX activity was measured by monitoring the oxidation of reduced cytochrome *c* by spectrophotometric analysis at 550 nm for 2 min at 37°C using a BioSpec-1601 spectrophotometer (Shimadzu, Kyoto, Japan). COX activity was determined by measuring the decrease in absorbance of ferrocytochrome *c* caused by its oxidation to ferricytochrome *c* by COX.

Transient transfection. Transient transfection of CEM/Neo cells was performed using SuperFect Transfection Reagent from QIAGEN GmbH (Hilden, Germany). Briefly, 3 μg of pIRES (empty vector), pcDNA3-Bcl-2 or mutant Bcl-2 plasmids was added to 20 μl of the SuperFect Transfection Reagent and transfection was carried out as recommended by the vendor. Bcl-2 expression was detected from cell lysates at various posttransfection time points by western blotting using a primary mouse monoclonal anti-Bcl-2 antibody at 1 : 1000 dilution (Santa Cruz Biotechnology, Santa Cruz, CA, USA) and a secondary HRP-conjugated goat anti-mouse IgG at 1 : 5000 dilution (Pierce, Illinois, IL, USA).

RNA interference. CEM/Bcl-2 cells were transfected 48 h and 72 h before experiments with 0.2 μM Bcl-2-specific siRNA (QIAGEN GmbH, Germany) or scrambled siRNA duplexes using Oligofectamine reagent according to the manufacturer's instructions (Invitrogen, Carlsbad, CA, USA). The expression level of Bcl-2 was confirmed by western blotting using antibodies as described previously for the detection of Bcl-2.

O_2^- measurement by lucigenin. A lucigenin-based chemiluminescence assay was used for measuring intracellular O_2^- as described previously.[19] Chemiluminescence was monitored using a Berthold Sirius Luminometer (Berthold detection systems GmbH, Bleichstrabe, Pforzheim, Germany). The assay was also used to detect the O_2^- level in isolated mitochondria in some instances. Data are described as RLUs/s per μg of protein.

O_2^- measurement by MitoSOX Red. The O_2^- production from mitochondria was also specifically monitored by MitoSOX Red (Invitrogen), which is a fluorescent probe targeted to the mitochondria and highly susceptible to oxidation by O_2^-. Briefly, 1×10^6 cells were incubated with 10 μM MitoSOX Red reagent for 15 min at 37°C. The cells were washed twice with 1 $\times$ PBS and immediately analyzed in Epic Profile flow cytometer (Beckman Coulter Inc., Fullerton, CA, USA) with excitation set at 510 nm. Data were analyzed for 10 000 events using WinMDI software (http://facs.scripps.edu/software.html).

Mitochondrial transmembrane potential determination. Potential-sensitive probe 3,3′dihexyloxacarbocyanine iodide ($DiOC_6$) was used to measure mitochondrial transmembrane potential as described previously.[37] Briefly, 1×10^6 cells were incubated with 40 nM $DiOC_6$ for 15 min at 37°C. At least 10 000 events were analyzed by flow cytometry with excitation set at 488 nm.

Coimmunofluorescence using confocal microscopy. The MitoTracker probe was added at 1 : 2000 dilution to live cells for the identification of mitochondria (Invitrogen). The cells were incubated for 20 min at RT and were washed thrice with PBS. The cells were fixed with 4% (v/v) paraformaldehyde for 20 min at RT and washed thrice with PBS before being permeabilized with 0.2% (v/v) Triton X-100 for 10 min at RT. The fixed and permeabilized cells were then washed thrice with PBS before being blocked with 1% (w/v) BSA for 30 min at RT. The cells were again washed thrice to remove excess blocking buffer. Primary antibodies in blocking buffer (1% (w/v) BSA in 1 $\times$ PBS) were added to both CEM/Neo and CEM/Bcl-2 cells at 1 : 50–1 : 200 dilution to a final concentration of 1–5 μg/ml. The cells were incubated for 1 h at RT. Thereafter, the cells were washed thrice with PBS to remove excess antibodies before being added to secondary antibodies conjugated with either Rhodamine Red (Molecular Probes, Invitrogen, Carlsbad, CA, USA) or FITC (Dako, Glostrup, Denmark) at 1 : 1000 or 1 : 50 dilution, respectively. The cells were incubated for 1 h at RT and washed thrice with PBS to remove excess antibodies. Each sample was then mounted onto a microscope glass slide (Livingstone, Rosbery, New South Wales, Australia) with 10 μl of FluorSave Reagent (Calbiochem, Merck KGaA, Darmstadt, Germany). The fluorochromes were subjected to excitation wavelengths of 488 nm at 1 mW HeNe Green and 543 nm at 40 mW argon for FITC and Rhodamine Red, respectively, using an Olympus IX81 FluoView 500 confocal microscope (Hamburg, Germany).

Coimmunoprecipitation and western blotting. Cells were lysed with 2 ml co-IP buffer (1% (v/v) NP40, 50 mM Tris, 150 mM NaCl at pH 7.4) and incubated on ice for 30 min with occasional mixing. The lysate was then centrifuged at 10 000 $\times$ *g* for 10 min at 4°C. Protein determination assay was carried out. An equal amount of protein was used for each sample, which was then added with BSA to reduce nonspecific binding, and subsequently added with 2 μg antibody targeting the bait. The samples were incubated overnight at 4°C with rocking. Thereafter, 30 μl of Protein A-Agarose beads was added (Santa Cruz Biotechnology) and incubated for 2 h at 4°C. The samples were centrifuged at 10 000 $\times$ *g* for 75 s at 4°C and the beads were washed with 1 ml co-IP buffer and centrifuged as described previously. Washing was repeated thrice. The pull-down fractions were then added with 40 μl of loading buffer. Proteins were analyzed and resolved on a 12% (v/v) acrylamide resolving gel, subjected to SDS-PAGE. The resolved proteins were then transferred onto a polyvinyl difluoride membrane by the semi-dry transfer method using the Hoefer TE 77 semi-dry transfer unit (Amersham Biosciences, Piscataway, NJ, USA). The membrane was subsequently blocked with 5% (w/v) fat-free milk in Tris-buffered saline containing 0.05% (v/v) Tween 20 (TBST) for 1 h. After three washes with TBST to remove excess milk, the membrane was probed for the protein of interest with the relevant primary antibody in 5% (w/v) BSA in TBST at 4°C for 1–2 h. The membrane was subsequently subjected to three washes with TBST to remove unbound primary antibody and probed again with the appropriate HRP-conjugated secondary antibody in TBST containing 1% (w/v) fat-free milk for 1 h at RT. After three washes with TBST to remove any excess unbound secondary antibody, the desired proteins were detected with a Kodak Biomax MR X-ray film (Sigma-Aldrich) by enhanced chemiluminescence using the SuperSignal Chemiluminescent Substrate (Pierce). The primary and secondary antibodies used for detection by western blot analysis were applied at 1 : 1000 and 1 : 5000 dilutions, respectively.

Blue Native PAGE. For immunoblot analysis of one-dimensional native gels, mitochondrial fractions were solubilized with *n*-dodecyl-β-D-maltoside or digitonin found in the NativePAGE Sample Prep Kit (Invitrogen) and carried out as described by the vendor and subsequently resolved on blue native 4–16% Bis–Tris polyacrylamide gels (Invitrogen). Electroblotting and immunodetection were routinely performed as described earlier.

Bioinformatics and mutagenesis. Structural homology analysis was carried out using the DaliLite server available on the web. Mutagenesis of *bcl-2* was performed using the Quikchange Site-Directed Mutagenesis Kit (Stratagene, La Jolla, CA, USA). Point mutants and the domain mutant of Bcl-2 were generated as recommended by the vendor. Briefly, forward and reverse primers harboring the sequence for the respective point mutation were generated. Using the nonstrand-displacing action of *PfuTurbo* DNA polymerase, these mutagenic primers were then used in a PCR reaction, together with the plasmid containing the target gene and the intended site of mutation. The methylated, nonmutated parental DNA template was subsequently digested with *Dpn* I, leaving behind the daughter plasmid incorporated with the desired mutation of the target gene. Mutations were confirmed by sequencing, after transformation, selection and restriction digest.

Acknowledgements. This work is supported by grants from the Biomedical Research Council of Singapore (R-185–000–164–305), and the NUS Academic Research Fund, Singapore (R-185–000–136–112) to SP. The NPC cell lines were gifts from Lo Kwok-wai (The Chinese University of Hong Kong) and Hsieh Wen-son (John Hopkins Medical Institute, USA). We thank Thomas Loh (National University Hospital, Singapore) and Jayshree Hirpara (National University of Singapore) for

providing the lymphoma samples and for excellent technical assistance with the samples, respectively. ZXC designed, performed the experiments and wrote the paper. SP designed the experiments and wrote the paper. Both authors discussed the results and commented on the paper.

1. Matoba S, Kang JG, Patino WD, Wragg A, Boehm M, Gavrilova O *et al.* p53 regulates mitochondrial respiration. *Science* 2006; **312**: 1650–1653.
2. Fukuda R, Zhang H, Kim JW, Shimoda L, Dang CV, Semenza GL. HIF-1 regulates cytochrome oxidase subunits to optimize efficiency of respiration in hypoxic cells. *Cell* 2007; **129**: 111–122.
3. Dowhan W, Bibus CR, Schatz G. The cytoplasmically-made subunit IV is necessary for assembly of cytochrome c oxidase in yeast. *EMBO J* 1985; **4**: 179–184.
4. Trueblood CE, Poyton RO. Differential effectiveness of yeast cytochrome c oxidase subunit genes results from differences in expression not function. *Mol Cell Biol* 1987; **7**: 3520–3526.
5. Burke PV, Raitt DC, Allen LA, Kellogg EA, Poyton RO. Effects of oxygen concentration on the expression of cytochrome c and cytochrome c oxidase genes in yeast. *J Biol Chem* 1997; **272**: 14705–14712.
6. Bunn HF, Poyton RO. Oxygen sensing and molecular adaptation to hypoxia. *Physiol Rev* 1996; **76**: 839–885.
7. Dagsgaard C, Taylor LE, O'Brien KM, Poyton RO. Effects of anoxia and the mitochondrion on expression of aerobic nuclear COX genes in yeast: evidence for a signaling pathway from the mitochondrial genome to the nucleus. *J Biol Chem* 2001; **276**: 7593–7601.
8. Poyton RO, Burke PV. Oxygen regulated transcription of cytochrome c and cytochrome c oxidase genes in yeast. *Biochim Biophys Acta* 1992; **1101**: 252–256.
9. Williams SL, Valnot I, Rustin P, Taanman JW. Cytochrome c oxidase subassemblies in fibroblast cultures from patients carrying mutations in COX10, SCO1, or SURF1. *J Biol Chem* 2004; **279**: 7462–7469.
10. Nijtmans LG, Taanman JW, Muijsers AO, Speijer D, Van den Bogert C. Assembly of cytochrome-c oxidase in cultured human cells. *Eur J Biochem* 1998; **254**: 389–394.
11. Wu H, Rao GN, Dai B, Singh P. Autocrine gastrins in colon cancer cells up-regulate cytochrome c oxidase Vb and down-regulate efflux of cytochrome c and activation of caspase-3. *J Biol Chem* 2000; **275**: 32491–32498.
12. Wu H, Owlia A, Singh P. Precursor peptide progastrin(1–80) reduces apoptosis of intestinal epithelial cells and upregulates cytochrome c oxidase Vb levels and synthesis of ATP. *Am J Physiol Gastrointest Liver Physiol* 2003; **285**: G1097–G1110.
13. Fu WN, Shang C, Huang DF, Xu ZM, Sun XH, Sun KL. Average-12.9 chromosome imbalances coupling with 15 differential expression genes possibly involved in the carcinogenesis, progression and metastasis of supraglottic laryngeal squamous cell cancer. *Zhonghua Yi Xue Yi Chuan Xue Za Zhi* 2006; **23**: 7–11.
14. Bini L, Magi B, Marzocchi B, Arcuri F, Tripodi S, Cintorino M *et al.* Protein expression profiles in human breast ductal carcinoma and histologically normal tissue. *Electrophoresis* 1997; **18**: 2832–2841.
15. Melis R, White R. Characterization of colonic polyps by two-dimensional gel electrophoresis. *Electrophoresis* 1999; **20**: 1055–1064.
16. Herrmann PC, Gillespie JW, Charboneau L, Bichsel VE, Paweletz CP, Calvert VS *et al.* Mitochondrial proteome: altered cytochrome c oxidase subunit levels in prostate cancer. *Proteomics* 2003; **3**: 1801–1810.
17. Vijayasarathy C, Biunno I, Lenka N, Yang M, Basu A, Hall IP *et al.* Variations in the subunit content and catalytic activity of the cytochrome c oxidase complex from different tissues and different cardiac compartments. *Biochim Biophys Acta* 1998; **1371**: 71–82.
18. Campian JL, Gao X, Qian M, Eaton JW. Cytochrome C oxidase activity and oxygen tolerance. *J Biol Chem* 2007; **282**: 12430–12438.
19. Clement MV, Stamenkovic I. Superoxide anion is a natural inhibitor of FAS-mediated cell death. *Embo J* 1996; **15**: 216–225.
20. Clement MV, Hirpara JL, Pervaiz S. Decrease in intracellular superoxide sensitizes Bcl-2-overexpressing tumor cells to receptor and drug-induced apoptosis independent of the mitochondria. *Cell Death Differ* 2003; **10**: 1273–1285.
21. Piantadosi CA, Suliman HB. Mitochondrial transcription factor A induction by redox activation of nuclear respiratory factor 1. *J Biol Chem* 2006; **281**: 324–333.
22. Hirai I, Wang HG. Survival-factor-induced phosphorylation of Bad results in its dissociation from Bcl-x(L) but not Bcl-2. *Biochem J* 2001; **359**: 345–352.
23. Harris MH, Thompson CB. The role of the Bcl-2 family in the regulation of outer mitochondrial membrane permeability. *Cell Death Differ* 2000; **7**: 1182–1191.
24. Steinman HM. The Bcl-2 oncoprotein functions as a pro-oxidant. *J Biol Chem* 1995; **270**: 3487–3490.
25. Chen ZX, Pervaiz S. Bcl-2 induces pro-oxidant state by engaging mitochondrial respiration in tumor cells. *Cell Death Differ* 2007; **14**: 1617–1627.
26. Frezza C, Cipolat S, Scorrano L. Organelle isolation: functional mitochondria from mouse liver, muscle and cultured fibroblasts. *Nat Protoc* 2007; **2**: 287–295.
27. Su X, Dowhan W. Translational regulation of nuclear gene COX4 expression by mitochondrial content of phosphatidylglycerol and cardiolipin in Saccharomyces cerevisiae. *Mol Cell Biol* 2006; **26**: 743–753.
28. Brix J, Rudiger S, Bukau B, Schneider-Mergener J, Pfanner N. Distribution of binding sequences for the mitochondrial import receptors Tom20, Tom22, and Tom70 in a presequence-carrying preprotein and a non-cleavable preprotein. *J Biol Chem* 1999; **274**: 16522–16530.
29. Motz C, Martin H, Krimmer T, Rassow J. Bcl-2 and porin follow different pathways of TOM-dependent insertion into the mitochondrial outer membrane. *J Mol Biol* 2002; **323**: 729–738.
30. Yin XM, Oltvai ZN, Korsmeyer SJ. BH1 and BH2 domains of Bcl-2 are required for inhibition of apoptosis and heterodimerization with Bax. *Nature* 1994; **369**: 321–323.
31. Wright RM, Poyton RO. Release of two Saccharomyces cerevisiae cytochrome genes, COX6 and CYC1, from glucose repression requires the SNF1 and SSN6 gene products. *Mol Cell Biol* 1990; **10**: 1297–1300.
32. Wright RM, Rosenzweig B, Poyton RO. Organization and expression of the COX6 genetic locus in Saccharomyces cerevisiae: multiple mRNAs with different 3′ termini are transcribed from COX6 and regulated differentially. *Nucleic Acids Res* 1989; **17**: 1103–1120.
33. Deng X, Gao F, Flagg T, Anderson J, May WS. Bcl2's flexible loop domain regulates p53 binding and survival. *Mol Cell Biol* 2006; **26**: 4421–4434.
34. Gao S, Chen J, Brodsky SV, Huang H, Adler S, Lee JH *et al.* Docking of endothelial nitric oxide synthase (eNOS) to the mitochondrial outer membrane: a pentabasic amino acid sequence in the autoinhibitory domain of eNOS targets a proteinase K-cleavable peptide on the cytoplasmic face of mitochondria. *J Biol Chem* 2004; **279**: 15968–15974.
35. Krahenbuhl S, Chang M, Brass EP, Hoppel CL. Decreased activities of ubiquinol:ferricytochrome c oxidoreductase (complex III) and ferrocytochrome c:oxygen oxidoreductase (complex IV) in liver mitochondria from rats with hydroxycobalamin [c-lactam]-induced methylmalonic aciduria. *J Biol Chem* 1991; **266**: 20998–21003.
36. Daley E, Wilkie D, Loesch A, Hargreaves IP, Kendall DA, Pilkington GJ *et al.* Chlorimipramine: a novel anticancer agent with a mitochondrial target. *Biochem Biophys Res Commun* 2005; **328**: 623–632.
37. Hirpara JL, Seyed MA, Loh KW, Dong H, Kini RM, Pervaiz S. Induction of mitochondrial permeability transition and cytochrome C release in the absence of caspase activation is insufficient for effective apoptosis in human leukemia cells. *Blood* 2000; **95**: 1773–1780.

Supplementary Information accompanies the paper on Cell Death and Differentiation website (http://www.nature.com/cdd)